

Bond Dissociation Energy in Trifluoride Ion

Alexander Artau,[†] Katrina Emilia Nizzi,^{‡,§} Brian T. Hill,^{†,||} Lee S. Sunderlin,^{*,‡} and Paul G. Wenthold^{*,†}

Contribution from the Department of Chemistry, Purdue University, West Lafayette, Indiana 47907-1393, and The Department of Chemistry and Biochemistry, Northern Illinois University, DeKalb, Illinois 60115-2862

Received May 11, 2000

Abstract: The bond dissociation energies in F_3^- are determined from energy-resolved collision-induced dissociation cross sections measurements in two tandem mass spectrometers. The gas-phase F_2-F^- bond dissociation energy is measured to be 1.02 ± 0.11 eV, and the energy for dissociation to $F + F_2^-$ is 0.28 ± 0.07 eV higher. After accounting for solvation energies, it is shown that the F_3^- is not expected to be stable with respect to dissociation in aqueous solution. Last, from the spectroscopic parameters, it is deduced that F_2^- formation is favored at high energies, in agreement with experimental results.

The trihalide anions X_3^- ($X = F, Cl, Br, \text{ and } I$) are prototypical examples of hypervalent bonding, with 10 electrons in the valence shell of the central atoms. Because of the hypervalent bonding, the ions Cl_3^- , Br_3^- , and I_3^- have all been well studied, using a wide range of experimental techniques. However, the trifluoride ion, F_3^- , is not well characterized because it has, until recently, only been observed at cryogenic temperatures in a rare gas matrix.^{1,2} Thus, for example, whereas the bond strengths in the other three trihalides have been measured both in the gas phase^{3,4} and in solution,³ the bond strength of F_3^- is not known.

Computational studies of the bonding properties of F_3^- have been carried out at very high levels of theory, but have proven to be challenging.^{5–8} Even with large basis sets, the theoretical values for the bond dissociation energy for formation of $F^- + F_2$ range from 53 kJ/mol at the MCSCF level of theory⁷ to 197 kJ/mol from BLYP calculations.⁷ At the highest levels of theory (CCSD(T)/TZ2Pf+),⁵ the bond dissociation energy for the gaseous ion is calculated to be 103 kJ/mol. Therefore, the F_3^- ion is predicted to be stable with respect to dissociation in the gas phase, which would imply that the inability to generate the ion in solution is a consequence of solvent effects.⁸

In agreement with the theoretical predictions, Tuinman et al.⁹ recently reported that the gaseous trifluoride ion is sufficiently stable to survive the source conditions of a mass spectrometer.

[†] Purdue University.

[‡] Northern Illinois University.

[§] Present address: Purdue University.

^{||} Present address: The Ohio State University, 100 West 18th Avenue, Columbus, OH, 43210-1185.

(1) Ault, B. S.; Andrews, L. *J. Am. Chem. Soc.* **1976**, *98*, 1591–1593.

(2) Ault, B. S.; Andrews, L. *Inorg. Chem.* **1977**, *16*, 2024–2028.

(3) Nizzi, K. E.; Pommerening, C. A.; Sunderlin, L. S. *J. Phys. Chem. A* **1998**, *102*, 7674–7679.

(4) Do, K.; Klein, T. P.; Pommerening, C. A.; Sunderlin, L. S. *J. Am. Soc. Mass Spectrom.* **1997**, *8*, 688–696.

(5) Heard, G. L.; Marsden, C. J.; Scuseria, G. E. *J. Phys. Chem.* **1992**, *96*, 4359–4366.

(6) Mota, F.; Novoa, J. J. *J. Chem. Phys.* **1996**, *105*, 8777–8784.

(7) Malcolm, N. O. J.; McDouall, J. J. W. *J. Phys. Chem.* **1996**, *100*, 10131–10134.

(8) Ogawa, Y.; Takahashi, O.; Kikuchi, O. *Chem. Phys. Lett.* **1998**, *424*, 285–292.

(9) Tuinman, A. A.; Gakh, A. A.; Hinde, R. J.; Compton, R. N. *J. Am. Chem. Soc.* **1999**, *121*, 8397–8398.

Electron-capture mass spectrometry of F_2 gives mainly F^- and F_2^- , but F_3^- is also observed as a minor product. Low-energy collision-induced dissociation of trifluoride ion with an argon target gas produces F^- and F_2^- as ionic fragments (reaction 1). At a collision energy of 25 eV in the laboratory frame (10.3 eV center-of-mass), F_2^- is the major fragment observed.⁹ This result is somewhat surprising because reaction 1a is energetically favored over reaction 1b by ~ 0.4 eV.¹⁰



In recent years, we have been investigating the bond dissociation energies in difluoride¹¹ and trihalide^{3,4} ions. Inspired by the results of Tuinman, et al.,⁹ we sought to extend these studies by measuring the bond dissociation energies in F_3^- . Here we report the determination of the bond dissociation energies of F_3^- as measured using energy-resolved collision-induced dissociation measurements. From the difference between the two bond dissociation energies, we calculate an electron affinity for F_2 that is in good agreement with the previously reported values. Last, we show that the preference for the formation of F_2^- upon collision-induced dissociation at higher energies is a result of statistical effects in the transition states for the two channels.

Experimental Section

The experiments were carried out using the guided-ion beam instruments at Purdue University and Northern Illinois University (NIU). Detailed explanations of these instruments and the experimental procedures have been given previously.^{3,4,12} At both institutions, ions are generated using electron ionization in a flowing afterglow. The pressure and flow rate of the helium buffer gas in the $1 \text{ m} \times 7.3 \text{ cm}$ (i.d.) flow reactor at Purdue were 0.4 Torr and 200 STP cm^3/s ,

(10) Bartmess, J. E. Negative Ion Thermochemical Data. In *NIST Chemistry WebBook*, NIST Standard Reference Database No. 69; Mallard, W. G., Linstrom, P. J., Eds.; National Institute of Standards and Technology: Gaithersburg, MD, 20899, February, 2000 (<http://webbook.nist.gov>).

(11) Wenthold, P. G.; Squires, R. R. *J. Phys. Chem.* **1995**, *99*, 2002–2005.

(12) Marinelli, P. J.; Paulino, J. A.; Sunderlin, L. S.; Wenthold, P. G.; Poutsma, J. C.; Squires, R. R. *Int. J. Mass Spectrom. Ion Processes* **1994**, *130*, 89–105.

respectively. The typical He pressure for the 92 cm \times 7.3 cm reactor at NIU was 0.4 Torr.⁴

The F_3^- ion was formed by the addition of F^- to F_2 . The F^- was formed by electron ionization of NF_3 and F_2 at Purdue and NIU, respectively. Other fluorine-containing ions, including F^- , F_2^- , and HF_2^- , were also observed. Under some source conditions, we observed a small amount of F_5^- (m/z 95), but unfortunately, the signal is too weak for subsequent studies. Care must be taken during these experiments to avoid the presence of water in the flow tube, because the water adduct of HF_2^- has the same nominal mass (m/z 57) as F_3^- .

Ions formed in the flowing afterglow are thermalized to ambient temperature by ca. 10^5 collisions with the helium buffer gas. More efficient stabilization of the metastable addition product was achieved by adding NF_3 or N_2O to the flow tube. The ions in the flow tube are sampled through a small orifice into the analyzer region of the instrument. The tandem mass spectrometer at NIU has a quadrupole–octopole–quadrupole configuration,^{3,4} while the instrument at Purdue is a triple quadrupole.¹² In both instruments, mass selection of F_3^- was carried out in the first quadrupole, collision-induced dissociation occurred in a gastight collision cell surrounding the second analyzer element, and products were mass-selected with the last quadrupole. The collision energy is adjusted by changing the DC offset voltage of the second element, with the absolute energy scale determined by a retarding potential analysis.¹³ A conversion dynode and electron multiplier operating in pulse-counting mode are used for ion detection.

Gas purities were as follows: He (99.995%), Ne (99%), NF_3 (99%), F_2 (99%).

Data Analysis. The data collection and analysis procedures used for CID threshold measurements have been described in detail.^{14,15} In these experiments, the yields of the particular CID product ions are monitored while the axial kinetic energy of the reactant ion is scanned. Product ion appearance curves are generated by plotting the CID cross sections versus the reactant ion–target collision energy in the center-of-mass (cm) frame, $E_{cm} = E_{lab}[m/(M + m)]$, where E_{lab} is the lab-frame energy, m is the mass of the neutral target, and M is the mass of the reactant ion. The energy axis origin is verified by retarding potential analysis, and the reactant ion kinetic energy distribution is generally found to have a near-Gaussian shape with a full width at half-maximum of 0.5–1.5 eV. Absolute cross sections for the formation of a single product from CID, σ , are calculated using the thin-target expression, $\sigma = I_p/INl$, where I_p and I are the measured intensities of the product and reactant ion signals, N is the number density of the target gas, and l is the effective collision path length for reaction (24 ± 4 cm at Purdue,¹² 13 ± 2^4 at NIU). At Purdue, phase incoherence between the quadrupolar fields in the triple quadrupole analyzer leads to oscillations in the apparent intensity of the reactant ion signal, but not the product ion signals, as the Q2 pole offset voltage is scanned. Accordingly, the intensity of the reactant ion beam is estimated to be equal to the maximum transmitted intensity in the region of the dissociation onset. This factor, as well as possible differences in the collection or detection efficiencies for the reactant and product ions, generally leads to a factor of 2 in the uncertainties in absolute cross sections and a $\pm 20\%$ uncertainty in relative cross sections. However, because of the high mass capabilities of the Purdue triple quadrupole, the mass discrimination is much more severe for ions below $m/z \sim 25$. To account for this, calibration experiments were carried out using $H_3O^+(H_2O)_2$ (m/z 55), which dissociates by loss of one or two water molecules to give products at m/z 37 and 19, respectively. It was found that the cross section for the formation of H_3O^+ as measured in the triple-quadrupole needed to be scaled by a factor of 1.6 in order to reproduce the literature ratio $[H_3O^+(H_2O)]/[H_3O^+]$ of 4.0 at a center-of-mass collision energy of 10 eV.¹⁶ Given that the masses of the H_3O^+ and $H_3O^+(H_2O)$ products are very similar to those of the F^- and F_2^- ions examined in this work, the cross sections of F^- have been scaled in the same manner. The relative

cross sections measured with the NIU instrument agree to within 10% with the literature results, and therefore do not need to be corrected.

The threshold energies for dissociation are determined by fitting the product ion appearance curves with the model function given by eq 2, which takes into account the rovibrational contributions to the total available energy.¹⁷

$$\sigma = \sigma_0 \sum_i P_D g_i (E + E_i - E_0)^n / E \quad (2)$$

In eq 2, E_0 is the dissociation threshold energy, E is the center-of-mass collision energy, σ_0 is a scaling factor, n is an adjustable parameter, i denotes reactant ion vibrational states having energy E_i and population g_i ($\sum g_i = 1$), and P_D is the probability for dissociation of the ion at a given energy.

The appearance curves are modeled using the CRUNCH data analysis program written by Armentrout, Ervin, and co-workers.^{13,17,18} The analysis utilizes an iterative procedure in which E_0 , σ_0 , and n are varied so as to minimize deviations between the data and the calculated cross sections in the steeply rising portion of the threshold region. A Doppler broadening function,¹⁹ which accounts for the random thermal motion of the target, and the kinetic energy distribution of the reactant ion approximated by a Gaussian function with a full width at half-maximum of 1.5 eV (lab frame) are also convoluted together with the calculated cross sections obtained with eq 2. The threshold energies obtained in this manner correspond to 0 K bond dissociation energies. The 298 K dissociation enthalpies are derived by combining the 0 K bond energy with the calculated difference in 0–298 K integrated heat capacities of the dissociation products and reactants, plus a PV work term ($RT = 2.5$ kJ/mol at 298 K).

The cross section model shown in eq 2 explicitly accounts for the possibility of kinetic shifts by incorporating a probability factor, P_D , for the dissociation of the ion at a given energy. Because of the small size of the ions and relatively low dissociation energies of F_3^- , dissociation of the collisionally activated ions occurs rapidly on the instrumental time scale ($\sim 3 \times 10^{-5}$ s) and is not subject to kinetic shifts. However, the reaction onsets likely suffer from competitive shifts due to the presence of a second dissociation pathway. The competition between the two channels is modeled by treating the competition as statistical.²⁰ Both channels are assumed to have loose, product-like transition states using the “phase space limit” approach described by Rodgers and Armentrout.²⁰ This issue will be discussed below.

Results and Discussion

Cross sections as a function of center-of-mass energy for the collision-induced dissociation of F_3^- with neon target gas measured at Purdue and at NIU are shown in Figure 1, a and b, respectively. Two products, F^- (m/z 19) and F_2^- (m/z 38), were observed in the dissociation. Excellent correspondence is observed between the data from the two instruments. The apparent onset for formation of F^- is slightly less than 1 eV, whereas that for F_2^- is higher by about 0.5 eV. Moreover, although the onset for formation of F^- is lower than that for F_2^- , at energies above ~ 3 eV the cross section for F_2^- is higher than that for F^- , as found by Tuinman et al.⁹

The bond dissociation energies for the channels can be determined by analysis of the energy-dependent collision cross sections for CID, as described above. Where available, experimentally known properties (Table 1) were utilized in the analysis.^{21–24} For the ν_2 mode in F_3^- , we use the extrapolated value of 260 cm^{-1} obtained by Heard et al.⁵ at the CCSD(T) level of theory. Rotational constants for F_3^- and F_2^- were

(13) Ervin, K. M.; Armentrout, P. B. *J. Chem. Phys.* **1985**, *83*, 166–189.

(14) Wenthold, P. G.; Squires, R. R. *J. Am. Chem. Soc.* **1994**, *116*, 6401.

(15) Sunderlin, L. S.; Wang, D.; Squires, R. R. *J. Am. Chem. Soc.* **1993**, *115*, 12060.

(16) Dalleska, N. F.; Honma, K.; Armentrout, P. B. *J. Am. Chem. Soc.* **1993**, *115*, 12125–12131.

(17) Schultz, R. H.; Crellin, K. C.; Armentrout, P. B. *J. Am. Chem. Soc.* **1991**, *113*, 8590–8601.

(18) Rodgers, M. T.; Ervin, K. M.; Armentrout, P. B. *J. Chem. Phys.* **1997**, *106*, 4499–4508.

(19) Chantry, P. J. *J. Chem. Phys.* **1971**, *55*, 2746.

(20) Rodgers, M. T.; Armentrout, P. B. *J. Chem. Phys.* **1998**, *109*, 1787–1800.

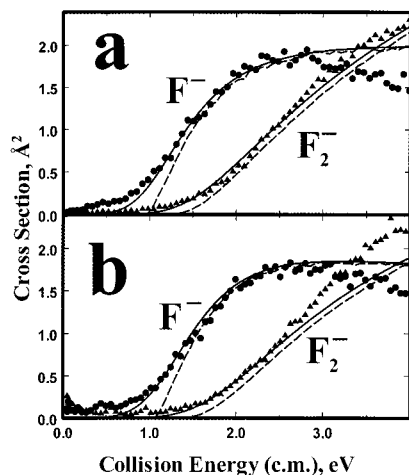


Figure 1. Cross sections for collision-induced dissociation of F_3^- measured at (a) Purdue University and (b) Northern Illinois University. The solid lines are calculated fits to the data, assuming statistical partitioning to give the products, and the dashed lines are nonconvoluted curves.

Table 1. Calculated and Measured Spectroscopic Constants for F_3^- , F_2^- , F_2 , and F^a

	B3LYP	MP2	QCISD(T)	exptl	exptl reference
F_3^-	-299.45989	-298.83623	-298.86225		
ν_1	439	406	396	461	1
ν_2	263	259	247		
ν_3	463	729	512	550	1
B_e	0.15	0.15	0.14		
F_2^-	-199.67468	-199.24950	-199.26385		
ν_1	358	484	449	460	22
B_e	0.44	0.48	0.47		
D_0	1.74	1.23	1.18	1.21	11
F_2	-199.53541	-199.12692	-199.14800		
ν_1	1022	934	831	916.64	21
B_e	0.90	0.87	0.84	0.890	21
$\alpha/4\pi\epsilon_0$	1.09	1.04	1.11	1.054	24
D_0	1.48	1.38	1.25	1.60	21
F^-	-99.87037	-99.66595	-99.66934		
F	-99.73950	-99.53707	-99.55020		
$\alpha/4\pi\epsilon_0$	0.43	0.41	0.44	0.557	23
$D_0(F_2-F^-)$	1.46	1.15	1.20	1.02 ± 0.11	this work
$D_0(F-F_2^-)$	1.19	1.29	1.27	1.30 ± 0.13	this work

^a Units: absolute energies in hartrees, frequencies and rotational constants in cm^{-1} , polarizabilities in \AA^3 , and bond dissociation energies in eV. All calculations were carried out using an aug-cc-pVDZ basis set.

obtained from molecular orbital calculations carried out in this work.²⁵ A comparison of the computational results from three different levels of theory is provided in Table 1. Of the computational methods examined, the QCISD(T) level provides the best agreement with the available experimental results. Therefore, QCISD(T)/aug-cc-pVDZ results are used for the rotational constants. The uncertainties in the calculated frequencies⁵ and rotational constants are estimated to be $\pm 10\%$.

Because the difference in the anharmonicities of the dissociation products may affect the branching ratio, they have been included in the analysis. For F_2 , the experimental anharmonicity of 11.24 cm^{-1} was used.²¹ The experimental anharmonicity for

F_2^- is not known but has been calculated to be 1.0 cm^{-1} using a multiconfiguration valence bond approach.²⁶ We have also carried out the fitting using values of 0 and 2.13 cm^{-1} (the Birge–Sponer estimate).²⁷ The F^- binding energies obtained using these three different values agree to within 0.03 eV. The reported value is the average of the three results, and a 0.015 eV contribution has been included in the uncertainty. The energy differences between the two channels using the three approaches agree to within 0.002 eV.

The threshold (ΔE_0) for reaction 1a is determined to be $0.98 \pm 0.13 \text{ eV}$ and $1.06 \pm 0.10 \text{ eV}$ from fits to the Purdue and NIU data, respectively. The difference between the thresholds for the two reaction channels is determined to be 0.25 ± 0.06 and $0.30 \pm 0.06 \text{ eV}$, respectively. The uncertainties include the standard deviations in parameters for the individual data sets, as well as the effects of the uncertainties in the calculated frequencies, potential mass discrimination (estimated at $\pm 20\%$ for either product), the uncertainty in the energy scale (estimated to be 0.15 eV in the lab frame), and an estimated 0.015 eV contribution due to uncertainty in the anharmonicity of F_2^- . The variation in parameters for individual data sets is the primary source of uncertainty in the overall threshold, and the possible mass discrimination is the dominant source of uncertainty in the difference between the thresholds. Experiments utilizing argon target produced lower quality data than those carried out using neon but gave quantitatively similar results.

After combining the results from the two instruments, we obtain a 0 K bond dissociation energy of $1.02 \pm 0.11 \text{ eV}$ and an energy difference between the two channels of $0.28 \pm 0.07 \text{ eV}$ (Table 1). Because the difference in the two thresholds is equal to the difference between the electron affinities (EAs) of F and F_2 , the present results can be combined with $EA(F) = 3.4012 \text{ eV}$ ²⁸ to give $EA(F_2) = 3.12 \pm 0.07 \text{ eV}$, in reasonable agreement with the previously reported values of 3.01 ± 0.07 ¹¹ and $3.08 \pm 0.10 \text{ eV}$.²⁹ The measured F_2-F^- bond dissociation energy is also in reasonable agreement with CCSD(T) (1.07 eV),⁵ MCSCF+MP2 (1.31 eV),⁶ QCISD(T) (1.15 eV), and MP2 (1.20 eV) calculations (Table 1). Significantly worse agreement is found for the simple CASSCF (0.53 eV)⁷ and B3LYP levels of theory (Table 1), the latter of which fails to correctly reproduce the relative energies of the two channels.

The reactant ion F_3^- initially is in the ground singlet electronic state. Collisional activation is expected to cause rotational and vibrational excitation, but not electronic excitation. Dissociation on the initial electronic surface leads without a barrier to the ground-state singlet products $F_2 + F^-$.³⁰ The other product

(25) Frisch, M. J.; Trucks, G. W.; Schlegel, H. B.; Scuseria, G. E.; Robb, M. A.; Cheeseman, J. R.; Zakrzewski, V. G.; Montgomery, J. A., Jr.; Stratmann, R. E.; Burant, J. C.; Dapprich, S.; Millam, J. M.; Daniels, A. D.; Kudin, K. N.; Strain, M. C.; Farkas, O.; Tomasi, J.; Barone, V.; Cossi, M.; Cammi, R.; Mennucci, B.; Pomelli, C.; Adamo, C.; Clifford, S.; Ochterski, J.; Petersson, G. A.; Ayala, P. Y.; Cui, Q.; Morokuma, K.; Malick, D. K.; Rabuck, A. D.; Raghavachari, K.; Foresman, J. B.; Cioslowski, J.; Ortiz, J. V.; Stefanov, B. B.; Liu, G.; Liashenko, A.; Piskorz, P.; Komaromi, I.; Gomperts, R.; Martin, R. L.; Fox, D. J.; Keith, T.; Al-laham, M. A.; Peng, C. Y.; Nanayakkara, A.; Gonzalez, C.; Challacombe, M.; Gill, P. M. W.; Johnson, B.; Chen, W.; Wong, M. W.; Andres, J. L.; Head-Gordon, M.; Replogle, E. S.; Pople, J. A. *Gaussian 98*, revision A.9; Gaussian Inc.: Pittsburgh, PA, 1998.

(26) Copesey, D. N.; Murrell, J. N.; Stamper, J. G. *Mol. Phys.* **1971**, *21*, 193–207.

(27) Atkins, P. *Physical Chemistry*; Freeman: New York, 1998.

(28) Blondel, C.; Cacciani, P.; Delsart, C.; Trainham, R. *Phys. Rev. A* **1989**, *40*, 3698.

(29) Ayala, J. A.; Wentworth, W. E.; Chen, E. C. M. *J. Phys. Chem.* **1981**, *85*, 768.

(30) Electronic state correlations during ion dissociation are discussed in: Armentrout, P. B.; Simons, J. *J. Am. Chem. Soc.* **1992**, *114*, 8627–8633.

(21) Huber, K. P.; Herzberg, G. Constants of Diatomic Molecules (data prepared by J. W. Gallagher and R. D. Johnson, III). In *NIST Chemistry WebBook*, NIST Standard Reference Database 69; Mallard, W. G., Linstrom, P. J., Eds.; National Institute of Standards and Technology: Gaithersburg, MD, 20899, February, 2000 (<http://webbook.nist.gov>).

(22) Howard, W. F., Jr.; Andrews, L. *J. Am. Chem. Soc.* **1973**, *95*, 3045–3046.

(23) Miller, T. M.; Bederson, B. *Adv. At. Mol. Phys.* **1977**, *13*, 1–55.

(24) Miller, K. J. *J. Am. Chem. Soc.* **1990**, *112*, 8533–8542.

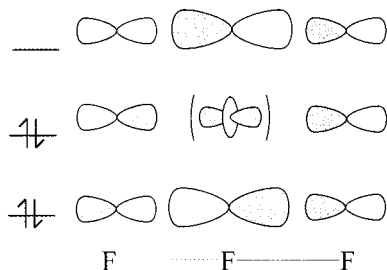


Figure 2. Molecular orbital diagram of F_3^- .

channel, $F + F_2^-$, correlates to singlet and triplet excited electronic states of F_3^- .³⁰ The singlet states can couple through their vibrational manifolds, but it is not obvious that this will be efficient on the dissociation time scale. However, statistical modeling of the CID data for I_3^- following the same procedure used here gives results in agreement with known thermochemistry,³¹ indicating that vibrationally mediated coupling between different electronic states is efficient when the energies of the two dissociation channels are reasonably close. Incomplete coupling between the electronic states would lead to too little F_2^- , which would give too low a value for $EA(F_2)$. The present value is slightly higher than the literature values, again suggesting that mixing is complete.

The preference for the formation of F_2^- at higher energies (>3 eV) noted by Tuinman and co-workers⁹ is qualitatively reproduced in the calculated fits of the data. Examination of the fitting parameters provides insight into the origins of this result. At low energies, the F^- channel is favored by enthalpy because the threshold for this channel is smaller in energy. However, the rotational and vibrational constants of F_2^- are lower than those for F_2 , resulting in a higher density of states for the F_2^- channel. Therefore, at high energies eq 1b becomes the dynamically favored reaction.

The bonding in hypervalent systems such as F_3^- has generally been explained using two models.³² The expanded octet model involves the promotion of an electron from a p orbital on the central atom to a d orbital. These two-half-filled orbitals are then used to bond to the two terminal atoms. The molecular orbital scheme is shown in Figure 2, where the $d\sigma$ orbital in parentheses is occupied. The promotion required is from an np orbital to an nd orbital for Cl, Br, and I ($n = 3, 4, \text{ or } 5$), but from a $2p$ orbital to a $3d$ orbital for F. Therefore, the promotion energy is much higher for F. The existence of Cl_3^- , Br_3^- , and I_3^- (but not F_3^-) in solution appears to support this model.

(31) Nizzi, K. E.; Sunderlin, L. S. **2000**, manuscript in preparation.

(32) Reed, A. E.; Schleyer, P. v. R. *J. Am. Chem. Soc.* **1990**, *112*, 1434–1445.

(33) Pimentel, G. C. *J. Chem. Phys.* **1951**, *19*, 446–448.

(34) Hach, R. J.; Rundle, R. E. *J. Am. Chem. Soc.* **1951**, *73*, 4321–4324.

(35) Cahill, P. A.; Dykstra, C. E.; Martin, J. C. *J. Am. Chem. Soc.* **1985**, *107*, 6359–6362.

(36) Magnusson, E. *J. Am. Chem. Soc.* **1990**, *112*, 7940–7951.

(37) Magnusson, E. *J. Am. Chem. Soc.* **1993**, *115*, 1051–1061.

(38) Marcus, Y. *Ion Properties*; Marcel Dekker: New York, 1997.

(39) Woods, T. L.; Garrels, R. M. *Thermodynamic Values at Low Temperature*; Oxford University Press: Oxford, 1987.

(40) Similarly small differences are seen in the solvation free energies of the rare gases, another set of nonpolar molecules (6 kJ/mol difference between He and Xe): Benson, B. B.; Krause, D. *J. Chem. Phys.* **1976**, *64*, 689–709.

(41) Christie, K. O. *J. Fluorine Chem.* **1995**, *71*, 149–150.

The three-center, four-electron (3C-4E) model^{33,34} assumes that the $d\sigma$ is not occupied; rather, the intermediate molecular orbital in Figure 2 is a nonbonding orbital localized on the terminal atoms with no contribution from the orbital in parentheses. Recent computational work has strongly supported this interpretation of the bonding.^{32,35–37} Since only p orbitals are involved, the 3C-4E bonding scheme predicts that trifluoride should not have a uniquely weak bond.

The 0 K gas-phase bond dissociation energies in the trihalide ions have now been measured as 98 ± 11 , 99 ± 5 ,³ 127 ± 7 ,³ and 126 ± 6 kJ/mol⁴ for $X = F, Cl, Br, \text{ and } I$, respectively, which correspond to 298 K bond dissociation enthalpies of 101, 100, 127, and 126, respectively. Although there is a small upward trend in these values, it is clear that the bond energies are not significantly different. This contradicts the expanded octet model and therefore provides strong experimental support for the 3C-4E model.

The bond strengths of the trihalide anions are much higher in the gas phase than in solution. This is due to differences between the solvation energies of X_3^- and $X^- + X_2$. According to the Born model,²⁷ ΔG_{solv} of an ion is inversely proportional to its ionic radius. The ionic radius of the F_3^- anion can be estimated by assuming the volume of F_3^- is 3 times that of F^- . Therefore, with $\Delta G_{\text{solv}}(F^-) = -510$ kJ/mol in water,³⁸ the free energy of solvation of F_3^- in water is estimated to be -350 kJ/mol. The free energy of solvation of F_2 can be estimated as 10 kJ/mol by extrapolation of the values for gaseous I_2 , Br_2 , and Cl_2 ($-3, 4, \text{ and } 7$ kJ/mol, respectively).^{39,40} Thus, the difference between $\Delta G_{\text{solv}}(F_3^-)$ and $\Delta G_{\text{solv}}(F^- + F_2)$ is roughly 150 kJ/mol.

The calculated spectroscopic parameters for F_3^- can be used to determine a gas-phase reaction entropy of $\Delta S(\text{eq 1a}) = 104.5$ J/mol K. This can be combined with the experimental bond energy, converted to ΔH_{298} , and the solvation free energy to give $\Delta G_{298}(\text{eq 1a}) = 72$ and -80 kJ/mol in the gas phase and aqueous solution, respectively. Therefore, $F_3^-(\text{aq})$ is not expected to be stable with respect to dissociation in aqueous solution.

According to the Born equation,²⁷ ΔG_{solv} is also proportional to $(1 - \epsilon_r^{-1})$, where ϵ_r is the relative permittivity of the solvent (ϵ_r for vacuum = 1). This can be combined with the above thermochemistry to estimate that F_3^- should be stable with respect to dissociation in solvents with ϵ_r values less than ~ 1.7 . Compounds with permittivities lower than 1.7 include He, Ne, Ar, Kr, H_2 , N_2 , O_2 , F_2 , and CF_4 . This explains why F_3^- could be observed in an Ar matrix,^{1,2} but could not be made as a $(CH_3)_4N^+$ salt in CH_3CN or CHF_3 .⁴¹ Interestingly, this implies that F_3^- can be prepared in environments such as liquid F_2 or CF_4 , which may allow more facile spectroscopic measurements on this unusual hypervalent anion.

Acknowledgment. This research was supported by the National Science Foundation (CHE-9985883) and by the American Society for Mass Spectrometry. Thanks also to the donors of the Petroleum Research Foundation, as administered by the American Chemical Society, for partial support of this work. We are grateful to Professors Peter Armentrout and Kent Ervin for providing the CRUNCH data analysis software and for useful discussions.

JA001613E